Available online at www.sciencedirect.com
ScienceDirect
Journal of Power Sources 166 (2007) 519–525
JOURNAL OF POWER SOURCES
www.elsevier.com/locate/jpowsour

Effect of adding sorbitol to the electroplating solution on the process of depositing lead on copper and the morphology of the film produced

J.L.P. Siqueira, I.A. Carlos *

Departamento de Química, Universidade Federal de São Carlos, C.P. 676, 13565-905 São Carlos (SP), Brazil

Received 20 September 2006; received in revised form 20 December 2006; accepted 21 December 2006
Available online 13 January 2007

Abstract

The electrodeposition of lead on to a copper substrate from a plumbite solution, 0.1 M $Pb(NO_3)_2$ + 0.2 M sorbitol + NaOH, was investigated over a range of concentrations of the hydroxide. Interactions between the copper electrode surface and the lead deposit were investigated by the voltammetric technique. From these experiments, it was concluded that underpotential deposition (upd) of lead does not occur on copper and that lead nucleation occurs as soon as deposition is operative from −0.78 V. Energy-dispersive X-ray spectroscopy (EDS) and scanning electron microscopy (SEM) of the lead films corroborates this result. Lead films obtained at −0.78 and −0.90 V were adherent and could be used as a support in battery plates, but this adhesion of lead to copper cannot be attributed to upd. SEM analysis showed that films produced at potentials down to −0.90 V were smooth and that this is the critical potential for a transition from dense to pyramidal or dendritic crystals patterns. The dendritic crystallites can be transformed into a high-purity lead powder.
© 2007 Elsevier B.V. All rights reserved.

Keywords: Lead electrodeposition; Copper substrate; Sorbitol; Voltammetry; Scanning electron microscopy; Energy-dispersive X-ray spectroscopy

1. Introduction

Recent research into the electrodeposition of lead has been stimulated not only by its potential for application in several technological areas, such as the production of high-purity active material for the lead-acid battery [1] and lead recycling [2–4], but also because the high toxicity of lead can create a serious health and environmental problem.

In this laboratory, we have studied lead deposition from alkaline baths containing glycerol or sorbitol [4–6]. Potentiodynamic experiments have shown that, in the presence of sorbitol, lead electrodeposition on to an electrode of 1010 steel is a nucleated process and that the plating process is more inhibited by sorbitol than by glycerol. Also, we found that the morphology was improved: when dendritic crystallites were observed, they were much smaller than those seen in the presence of glycerol. While the lead deposits on 1010 steel obtained with glycerol and sorbitol were non-adherent and could be transformed into high-purity lead powder [4,5], those obtained on copper from a bath containing glycerol showed good adhesion [6]. Thus, the substrate material was shown to be relevant for the adherence of lead deposited from an alkaline plating bath containing glycerol or sorbitol.

Numerous attempts have been made to reduce the mass of a lead-acid battery by replacing the heavy and costly lead grids with a lighter material.

Exide Technologies Industrial Energy has worked on the development, manufacturing and marketing of submarine propulsion batteries with low-density active materials and low-volume, high-conductivity copper negative grids [7].

Also, some authors have investigated the deposition of lead layers on the surfaces of various metal substrates in the lead-acid battery [8,9]. The compact lead layers formed on the surfaces of Al, Ti, Zr, Ni, Cu, aluminium alloys and stainless steels, as well as on steels and titanium alloys preliminarily plated with copper, characteristically have high porosity. Such lead films can be used in the lead-acid battery as positive electrodes as they allow high discharge current densities to be attained. The best electrochemical characteristics are exhibited by the film electrode obtained by lead-plating a fine copper grid.

Kolb and Gerisher [10] report that when there is a small difference in work function between the metal substrate and

* Corresponding author. Tel.: +55 16 33518067; fax: +55 16 33518350.
E-mail address: diac@power.ufscar.br (I.A. Carlos).

0378-7753/$ – see front matter © 2007 Elsevier B.V. All rights reserved.
doi:10.1016/j.jpowsour.2006.12.066

metal deposit, underpotential deposition (upd) is not observed. Despić and Pavlović [11] showed that deposition on substrates exhibiting strong interactions proceeds without marked nucleation effects.

On the other hand, Wu and Yau [12] have observed upd of Pb on a Cu(1 0 0) electrode surface in 0.1 M sulphuric acid containing 1 mM $Pb(ClO_4)_2$ and noted that the amount of lead deposited could influence the surface morphology, particularly the orientation and roughness of steps. Deposition of a small amount of Pb vastly decreased kink density and meanwhile caused step realignments in the (0 1 1) direction.

Brisard et al. [13,14] who studied underpotential deposition of lead on Cu(1 1 1) and on Cu(1 0 0) surfaces, observed that lead atoms are deposited by upd on these substrates. The only real difference in Pb upd on the two different Cu crystal faces was the absence of an ordered structure in the compact layer formed on Cu(1 0 0), versus the ordered structure observed on Cu(1 1 1). This difference appears to be related to a lower mobility of Pb adatoms due to the greater atomic corrugation of the (1 0 0) surface.

Dobson and co-workers [15] studied the epitaxial growth of lead on copper and observed lead growing in the Stranski–Krastanov mode on (1 1 1) copper. Ordered submonolayer structures were not observed in the lead growing on the copper substrate, but a substantial contraction in the lead nearest neighbor spacing (∼3%) was observed at a coverage of approximately one monolayer. It was suggested that the resulting strain in the overlayer might be responsible for the Stranski–Krastanov growth mode. Parallel epitaxial layers were formed by lead on copper.

Gewirth and co-workers [16] studied the structure of the Pb monolayer electrochemically deposited on Cu(1 1 1) in 0.1 M $HClO_4$, using in situ surface X-ray diffraction. The Pb monolayer forms an unrotated incommensurate hexagonal structure. The nearest neighbor spacing of the Pb monolayer is compressed continuously from 1.4 to 3.2% of the bulk spacing as the electrode potential is varied, with no apparent tendency to lock in.

Meanwhile, in this laboratory lead deposition on to a copper substrate has proved to be of interest, since the adhesion of the lead coating to this substrate is significant [6].

Motivated by the results obtained in our former experiments [4–6], in this paper the study of lead electrodeposition continues, with particular emphasis on investigation of the influence of the copper substrate on the adherence of the lead film and the influence of sorbitol additive on the deposition process and on the morphology of lead films intended to be used as a support in battery plates.

2. Experimental

All chemicals were analytical grade. Double-distilled water was used throughout. Each electrochemical experiment was performed in a non-cyanide bath containing 0.1 M $Pb(NO_3)_2$ + 0.2 M sorbitol + NaOH at various concentrations (0.40, 0.60, 0.80, 1.0 and 2.0 M). A Cu disk (0.3 cm^2), a Pt plate and a Hg/HgO/1 M NaOH electrode with an appropriate Lugging capillary were employed as working, auxiliary and reference electrodes, respectively. The Cu substrate, from Aldrich, was 99.99% pure. Immediately prior to the electrochemical measurements, the Cu working electrodes were ground with 600-emery paper and then rinsed with water. Potentiodynamic curves were recorded with a PAR model 366 potentiostat/galvanostat and a plotting recorder. Measurements of deposition and dissolution charges were recorded with an EG&G model 379 coulometer. All experiments were carried out at room temperature (25 °C). Scanning electron microscopy (SEM) micrographs were taken with Carl Zeiss (model DMS 940A) and Phillips (model XL 30 FEP) electron microscopes. Energy-dispersive X-ray spectroscopy (EDS) measurements were made with a Zeiss/Leica (model LEO, 440) EDS Si/Li, with Be ultrathin window.

3. Results and discussion

3.1. Electrodeposition of Pb on copper substrate

Fig. 1 shows voltammograms for the copper substrate in electrolytic solutions containing 0.1 M $Pb(NO_3)_2$ at various NaOH concentrations, all containing 0.2 M sorbitol. Potential values were referred to the Hg/HgO/1 M NaOH reference electrode. To facilitate reading of the deposition voltammograms, they are divided into regions: I, II, III and IV. In region I (inset in Fig. 1), two peaks (approximately −0.55 and −0.65 V) can be seen in the initial moments of the deposition process, with a small current density (∼0.30 mA cm^{-2}). These peaks are associated with copper oxide reduction [6,17]. In region II (see inset in Fig. 1), the wave (approximately −1.26 mA cm^{-2}, −0.80 V for 2.0 M NaOH) and a first cathodic peak (−1.8 mA cm^{-2}, −0.75 V; −2.09 mA cm^{-2}, 0.75 V; −1.08 mA cm^{-2}, −0.78 V, for 0.6 M, 0.8 M and 1.0 M NaOH, respectively), were attributed to an initial thin layer of lead deposited on the copper substrate after copper oxide reduction. The second cathodic peak (region III) refers to bulk lead deposition on top of the thin lead layer. The current density and potential of the second

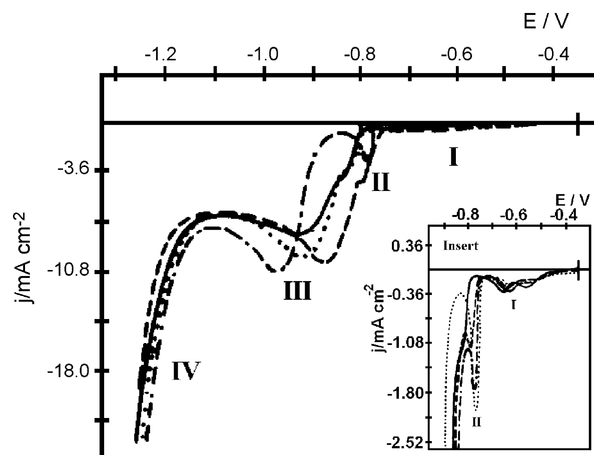

Fig. 1. Voltammetric curves for copper substrate in 0.1 M $Pb(NO_3)_2$ + 0.2 M sorbitol at various NaOH concentrations: (· – – ·) 0.6 M, (· · ·) 0.8 M, (– – –) 1.0 M and (—) 2.0 M at 10 mV s^{-1}. Potential (V) vs. Hg/HgO/1 M NaOH.

peak depend on the OH^- concentration ($-10.8\,mA\,cm^{-2}$, -0.98 V; $-9.72\,mA\,cm^{-2}$, -0.92 V; $-10.1\,mA\,cm^{-2}$, -0.86 V; $-7.92\,mA\,cm^{-2}$, -0.92 V, for 0.6 M, 0.8 M, 1.0 M and 2.0 M NaOH, respectively). Beyond this peak, the current density falls, indicating that the deposition is controlled by diffusion. Immediately after this region, the current density increases again, due to the hydrogen evolution reaction occurring in parallel with the reduction reactions of plumbite ions (region IV).

Examination of Fig. 1 shows that the lead-plating rate is affected kinetically by the hydroxide ion, since the current density in the second peak is not the same at all concentrations of OH^-. Moreover, this ion also affects the plating thermodynamically, since the potential of the second peak shifts to more negative values as the OH^- ion concentration falls, probably due to the decreasing conductivity of the solution. However, it can be seen that, in the bath containing 2.0 M OH^-, the deposition current density ($\sim$8 $mA\,cm^{-2}$) was the lowest in the region of second peak and also the deposition potential was more negative than in the bath containing 1.0 M OH^-. This is probably due to the concentration of free OH^- in the bath with 2.0 M NaOH being much higher than in any other bath, so that the deposition potential and current density are probably affected by a mechanism different from that operating at lower concentrations. The decomplexation of tetracoordinated Pb(II) compounds, for example, into singly coordinated ones at the metal/solution interface is probably affected by the free OH^- concentration, as suggested in Eq. (1):

$$Pb(OH)_4{}^{2-} \leftrightarrows Pb(OH)^+ + 3OH^- \quad (1)$$

Hence, the kinetics of lead deposition and the thermodynamic of plating would be affected.

The plating bath containing 0.1 M Pb^{2+}, 2.0 M NaOH and 0.2 M sorbitol proved to be the stablest and hence was chosen for further study of the deposition process.

Fig. 2 illustrates the effect of increasing the cathodic charge density (q_c) on the ratio of anodic to cathodic charge density (q_a/q_c). The lead films were obtained potentiodynamically from

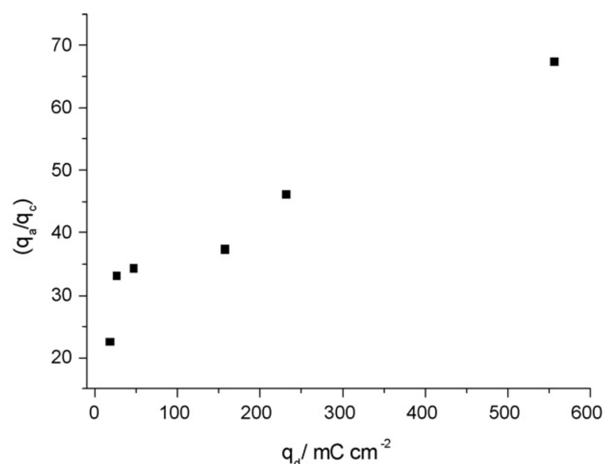

Fig. 2. Effect of increasing the deposition charge density (q_d) on the (q_a/q_c) ratio (q_a, anodic charge density) of lead electrodeposits obtained (at different deposition charges) from 0.1 M $Pb(NO_3)_2$ + 0.2 M sorbitol + 2.0M NaOH on copper substrate.

Table 1
Dissolution and deposition charges observed during lead voltammetric deposition on copper

$-E_f$ (V)	q_a ($mC\,cm^{-2}$)	q_c ($mC\,cm^{-2}$)	q_a/q_c (%)
0.86	3.98	17.63	22.60
0.90	8.44	25.43	33.20
0.95	15.96	46.35	34.43
1.12	58.64	156.70	37.42
1.15	106.61	230.90	46.17
1.2	374.82	555.70	67.45

-0.350 V to various final deposition potentials (E_f) and cathodic charge densities (Table 1). It can be seen that the anodic charge (q_a) increased rapidly as q_c increased and consequently the q_a/q_c ratio increased. Also, the anodic charge density increased as the sweep was taken to more negative potentials in the cathodic period, but not in proportion to the amount of lead deposited (Table 1 and Fig. 2).

Fig. 3 shows the voltammogram for a lead electrode in a solution containing 2.0 M NaOH + 0.2 M sorbitol. This voltammogram indicates the occurrence of two different processes: active dissolution and passivation. In region I of Fig. 3, Pb active dissolution occurs. In this region, the current density increases with potential in the anodic direction, up to peak a_1. Region II, which is characterized by a low current density relative to region I, is the passive region. The process of metal dissolution does occur in the region I. However, a surface of film starts to form, and beyond peak a_1 the rate of coating is sufficient to cause a significant fall in metal dissolution.

This result (Table 1) implies that the increase in the anodic charge density is not proportional to the amount of lead deposited, since passivation of lead film occurs during the anodic scan (Fig. 3). Moreover, it was observed that at the end of the anodic process, lead film obtained at various E_f (Table 1) had not dissolved completely, corroborating the values of q_a/q_c lower than 100%.

The q_a/q_c ratio for $E_f = -1.20$ V was higher ($\sim$67%) than that obtained for lead deposition on 1010 steel ($\sim$40%), since undercutting of lead film was not observed on copper.

It should be pointed out that this absence of undercutting of lead film is an indication of good adherence of the film to the copper substrate, corroborating results obtained previously in our laboratory [6].

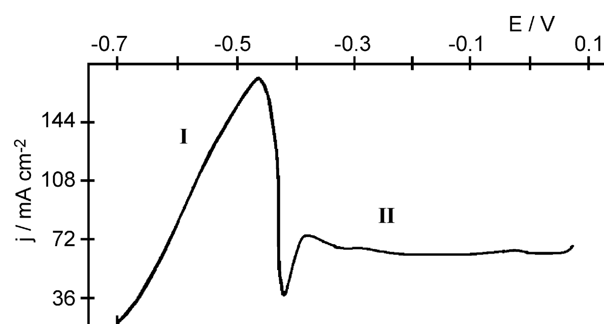

Fig. 3. Dissolution of lead electrode in solution containing 2.0 M NaOH and 0.2 M sorbitol, $\upsilon = 10\,mV\,s^{-1}$.

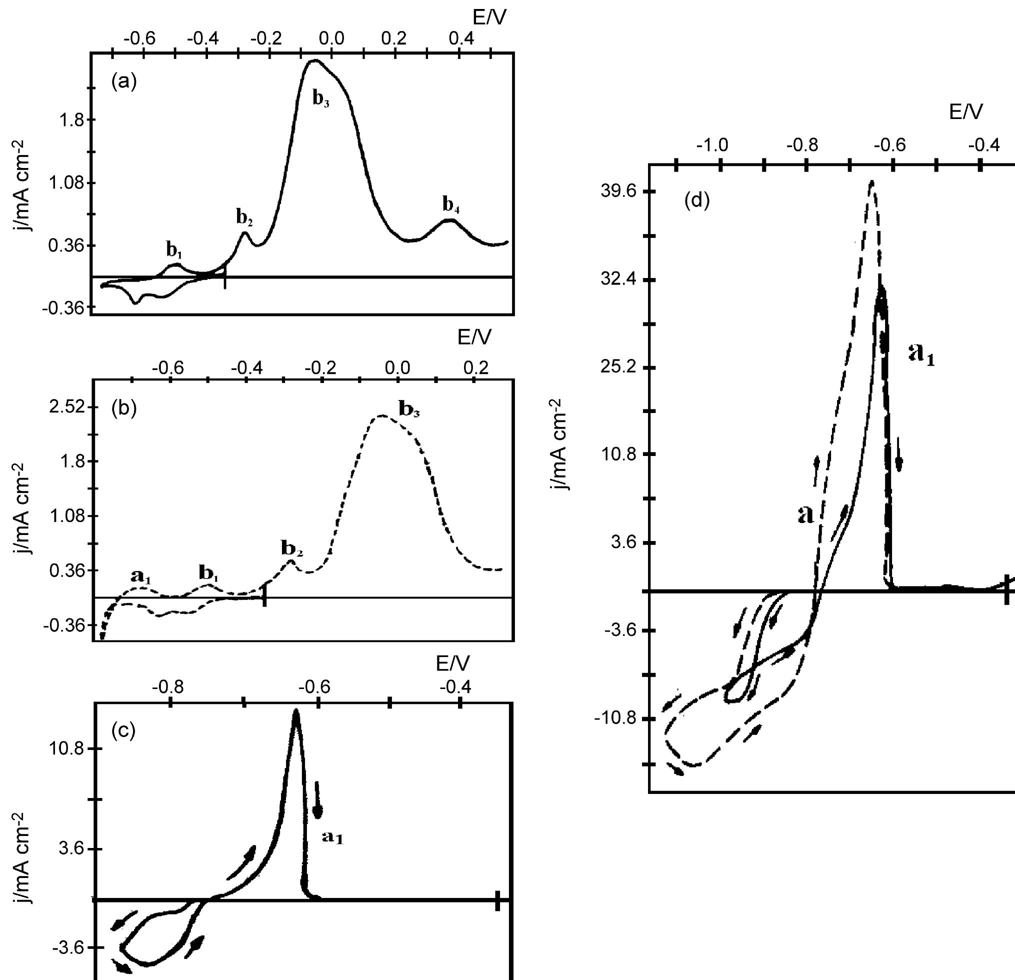

Fig. 4. Voltammetric curves (vs. Hg/HgO/1 M NaOH) for copper substrate in 0.1 M $Pb(NO_3)_2$ + 2.0 M NaOH + 0.2 M sorbitol—effect of varying the cathodic potential limit: (a) −0.750 V, (b) −0.780 V, (c) −0.860 V and (d) −0.99 V (solid line) and −1.2 V (dashed line); at 10 mV s^{-1}.

Fig. 4(a–d) shows stationary cyclic voltammograms with various lower limit potentials. The initial and upper potential values were −0.35 and −0.75 V, respectively. Potential values were referred to the Hg/HgO/1 M NaOH reference electrode. At potentials −0.780 (Fig. 4(b)) and −0.860 V (Fig. 4(c)), a crossover and a nucleation loop can be seen, respectively, which are not normal features of direct deposition, but are indeed expected in the case of nucleation [18]. In the anodic scan, a peak a_1 (−0.65 V) can be observed (Fig. 4(b and c)), which corresponds to lead dissolution. When the sweep was reversed at more positive potentials than −0.780 V (Fig. 4(a)), features of lead deposition and dissolution were not exhibited and the cathodic and anodic voltammograms obtained correspond to copper oxide reduction (region I) and formation: anodic peaks b_1 (−0.52 V), b_2 (−0.30 V), b_3 (−0.07 V) and b_4 (∼ +0.40 V, respectively.

Fig. 5(a and b) shows dissolution voltammograms for a copper electrode in a solutions containing 2.0 M NaOH and 2.0 M NaOH + 0.2 M sorbitol, respectively. It can be verified in Fig. 5(a), two anodic peaks b_1 and b_3, which correspond to formation of copper oxide and in Fig. 5(b), three anodic peaks (b_1, b_3 and b_4) and a shoulder b_2. The peaks b_1 and b_3 correspond to formation of copper oxide; the shoulder b_2 corresponds

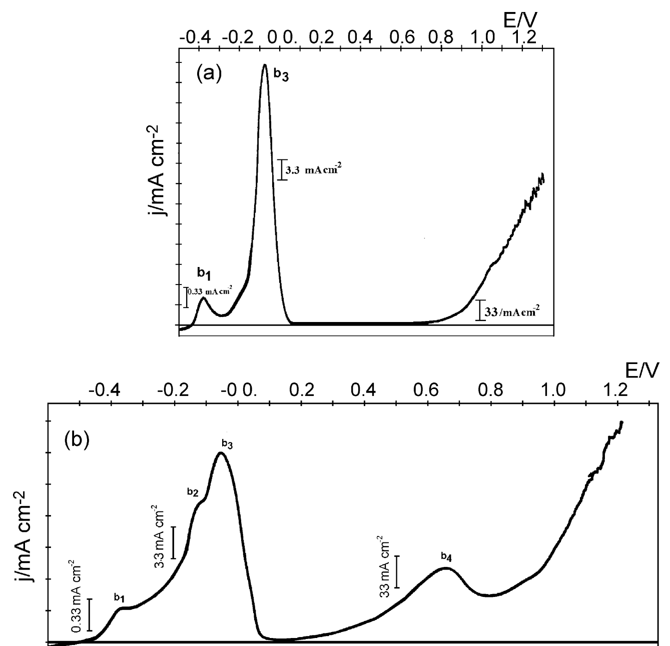

Fig. 5. Dissolution voltammograms for a copper electrode in solutions containing: (a) 2.0 M NaOH and (b) 2.0 M NaOH + 0.2 M sorbitol, at 10 mV s^{-1}.

probably to film that is formed only in the presence of sorbitol and peak b_4 to sorbitol oxidation.

Comparing Fig. 4(a) and Fig. 5(a and b), it can be inferred that in Fig. 4(a), the peaks b_1 and b_3 correspond to formation of copper oxide; the peak b_2 to film formed only in the presence of sorbitol and peak b_4 to sorbitol oxidation.

Thus, it can be inferred that the lead deposition process itself is absent at voltages less negative than approximately −0.780 V.

These results suggest that electrodeposition of lead on copper starts from −0.78 V and that nucleation occurs as soon as this deposition is operative, i.e., after copper oxide reduction on the copper substrate. Three-dimensional nucleation is therefore then a prerequisite of lead growth, since upd is absent [11].

When the sweep was reversed at the potential −0.990 V (Fig. 4(d), solid line) the current decreased, indicating that the deposition process was under mass transport control. Finally, a second nucleation process occurred when the sweep scan was reversed at −1.20 V (Fig. 4(d), dashed line), since an increase in current was observed.

Comparing the deposition potential E_d (approximately −0.780 V) with E_d of lead on 1010 steel (approximately −0.850 V) [5], it can be verified that they are not close. The work functions (ϕ) of iron, copper and lead are 4.50, 4.65 and 4.25 eV [19], respectively. The small $\Delta\phi$ value for Pb/Fe is not observed for Pb/Cu, corroborating the dissimilar deposition potentials of lead on 1010 steel and lead on copper. According to Kolb and Gerisher [10], when the $\Delta\phi$ value is significant, as is the case for lead on copper, underpotential deposition would be expected. However, these authors mention that metal monolayer deposition in aqueous solution on to a non-noble metal may yield ambiguous results, since anion adsorption is expected to interfere with monolayer adsorption. This is likely to be the case in the present study, since not only reduction of copper oxide but also adsorption of OH^- and sorbitol can occur.

It can be inferred from these results that in an alkaline lead bath with sorbitol, lead deposition on to copper has an advantage over lead on to 1010 steel [4,5], in that the lead film on the copper substrate was adherent. On the other hand, comparing lead deposition formed on to copper substrate in this bath with that in an alkaline-glycerol bath, it is found that the kinetics of the first is slower and the initial deposition potential more negative.

3.2. Morphology of lead electrodeposits on copper substrate

A morphological study was carried out by scanning electron microscopy to analyze the effects of fixing the hold potential in the different regions of the voltammetric deposition curve and to establish the relationship between the deposition potential and film morphology.

Fig. 6(a–d) show micrographs of the lead deposits, with the hold potential in the different regions of the voltammetric curve

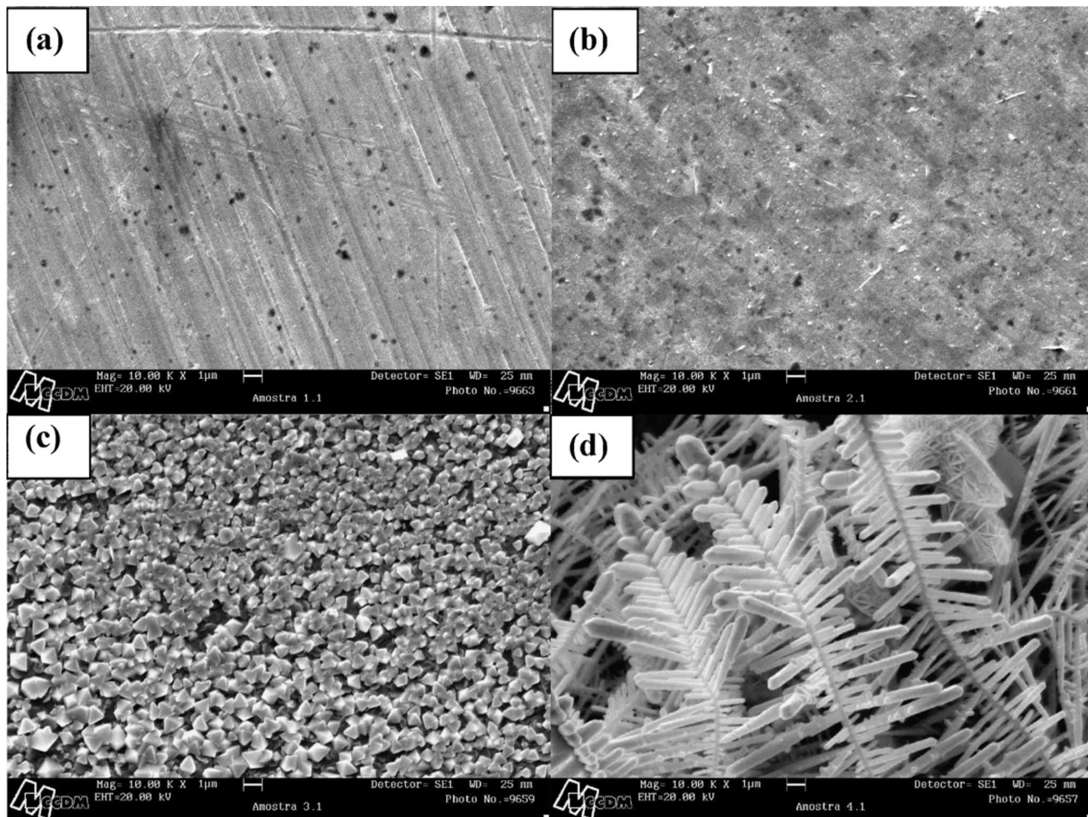

Fig. 6. SEM micrographs for lead films obtained in 0.1 M $Pb(NO_3)_2$ + 2.0 M NaOH + 0.2 M sorbitol. Potential sweeps from: (a) −0.350 to −0.780 V, (b) −0.350 to −0.900 V, (c) −0.350 to −1.00 and (d) −0.350 to −1.20 V, at 10 mV s^{-1} [10,000×]. ⊢⊣ 1 μm.

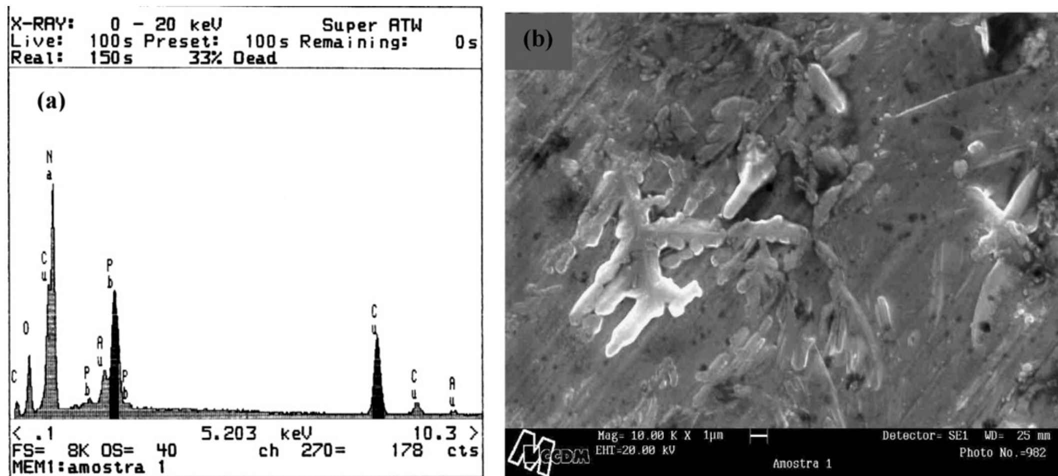

Fig. 7. EDS and SEM micrographs of deposits on copper obtained in 0.1M $Pb(NO_3)_2$ + 2.0M NaOH + 0.2M sorbitol. Potential sweeps from −0.350 to −0.780 V, held at −0.780 V until $q_c = 3.0\,C\,cm^{-2}$. ⊢⊣ 1 μm.

(Fig. 1), after scanning from −0.350 V to each hold potential. With a hold potential at −0.780 V, a thin lead layer covering the substrate was formed, Fig. 6(a), as can be seen more clearly in Fig. 7. Fig. 6(b–d) shows the micrographs for voltammetric deposition with hold potentials at −0.900, −1.00 and −1.20 V, respectively (see Fig. 1). At increasingly negative potentials, the lead deposit morphology changed from smooth (Fig. 6(a and b)), to pyramidal (Fig. 6(c)) and finally to dendritic (Fig. 6(d)). The smooth lead films (Fig. 6(a and b)), adhered to the copper substrate and thus can probably be used as support in battery plates, after ensuring that the hole-like defects observed on the SEM micrographs do not open the way for sulphuric acid to reach the copper substrate.

It was observed that under the dendritic crystallites, an adherent lead layer was formed on the copper substrate. The growth of three-dimensional dendritic lead deposits is probably a result of the contribution of mass transport to the control of the electrodeposition process, occurring at high negative deposition potentials [20]. As deposit growth is limited by mass transport (diffusion, migration, etc), an unstable situation develops and protruding parts of a surface grow faster, as they are more accessible [21]. This new phase (dendritic) corresponds to the second lead nucleation, corroborating results in Fig. 4(d) (dashed line). Moreover, it can be seen in Fig. 6(d) that, under these conditions, anisotropic growth of lead film occurred.

The film seen in Fig. 6, results from diffusion-controlled deposition, which produces well-defined small pyramidal crystals, whose average size, in the range 0.5–1 μm (Fig. 6(c)), is less than the average thickness of the diffusion layer (100 μm) [22,23] built up around the substrate electrode.

The lead layer formed in the initial moments of lead deposition was further investigated by SEM and EDS analysis (Fig. 7(a and b)). Lead film was laid down on copper substrate from −0.350 to −0.780 V, applying hold at −0.780 V until a charge density of $3.0\,C\,cm^{-2}$. It can be seen that the film is uniform and the percentage of lead is 33%. Hence, this result shows lead deposition just in the initial moments of deposition, corroborating the results in Fig. 4(b).

Finally, comparing the lead film morphology on 1010 steel with that on copper, from an alkaline-bath in the presence of sorbitol, it can be observed that in the first case the films obtained at −1.0 V were dendritic, while on copper the dendritic growth began at approximately −1.20 V. Moreover, the lead films obtained on 1010 steel were not adherent. Comparing the morphologies of lead films on copper obtained from alkaline-sorbitol and alkaline-glycerol baths, it should be noted that the films obtained at the start of deposition (approximately −0.90 V) from the sorbitol bath had a better appearance, inasmuch as it was smoother.

4. Conclusions

Lead alkaline plating solutions were successfully stabilized by the addition of sorbitol and no bath decomposition was observed during deposition. Potentiodynamic curves indicated that the lead deposition process is characterized by a wave or a first cathodic peak (thin lead film) and a second peak (bulk deposition). Lead deposition rate was high in the region of the second peak and controlled by mass transport. Also, it was shown that hydroxide anions affect the thermodynamics of the voltammetric deposition process. The q_a/q_c ratio for lead deposition on copper substrate ($E_f = -1.20$ V) was ∼67%. First and second nucleation of lead, respectively, on copper and on lead, were observed. SEM analysis showed that at increasingly negative potentials, the lead deposit morphology changed from smooth to pyramidal and finally to dendritic. The smooth lead film on copper substrate was adherent and thus may probably be used as support in battery plates. The adherence of lead film on a copper substrate cannot be attributed to upd. The dendritic lead film can be transformed into a high-purity lead powder. SEM and EDS analyses of the Pb films obtained in the initial moments of deposition indicated the occurrence of a uniform lead film containing 33% lead.

References

[1] D. Pavlov, J. Power Sources 42 (1993) 345.
[2] L. Doulakas, K. Novy, S. Stucki, Ch. Comninellis, Electrochim. Acta 46 (2000) 349.
[3] E. Exposito, J. Iniesta, J. Gonzaléz-Garcia, V. Montiel, A. Aldaz, J. Power Sources 92 (2001) 345.
[4] I.A. Carlos, M.A. Malaquias, M.M. Oizumi, T.T. Matsuo, J. Power Sources 92 (2001) 56.
[5] I.A. Carlos, J.L.P. Siqueira, G.A. Finazzi, M.R.H. de Almeida, J. Power Sources 117 (2003) 179.
[6] I.A. Carlos, J.L.P. Siqueira, T.T. Matsuo, M.R.H. de Almeida, J. Power Sources 132 (2004) 261.
[7] http://www.naval-technology.com/contractors/electrical/deutsche.
[8] L.A. Yolshina, V.Ya. Kudyakov, V.G. Zyryanov, J. Power Sources 65 (1997) 71–76.
[9] L.A. Yolshina, V.Ya. Kudyakov, V.G. Zyryanov, J. Power Sources 78 (1999) 84–87.
[10] D.M. Kolb, H. Gerischer, Surf. Sci. 51 (1975) 323.
[11] A.R. Despić, M.G. Pavlović, Electrochim. Acta 27 (1982) 1539.
[12] H.-C. Wu, S.-L. Yau, J. Phys. Chem. B 105 (2001) 6965–6971.
[13] G.M. Brisard, E. Zenati, H.A. Gasteiger, N.M. Marković, P.N. Ross Jr., Langmuir 11 (1996) 2221–2230.
[14] G.M. Brisard, E. Zenati, H.A. Gasteiger, N.M. Markovic', P.N. Ross Jr., Langmuir 13 (1997) 2390–2397.
[15] K.J. Rawlings, M.J. Gibson, P.J. Dobson, J. Phys. D: Appl. Phys. 11 (1978) 2059–2070.
[16] Y.S. Chu, I.K. Robinson, A.A. Gewirth, Phys. Rev. B 55 (12) (1997) 7945–7954.
[17] I.A. Carlos, M.R.H. de Almeida, L.L. Barbosa, R.M. Carlos, B.S. Lima-Neto, E.M.J.A. Pallone, J. Appl. Electrochem. 32 (2002) 763.
[18] S. Fletcher, C.S. Halliday, D. Gates, M. Westcott, T. Lwin, G. Nelson, J. Electroanal. Chem. 159 (1983) 267.
[19] R.C. Weast, Handbook of Chemistry and Physics, first ed., CRC Press, Florida, USA, 1990.
[20] A. Hernández Creus, P. Carro, S. González, A.E. Bolzan, R.C. Salvarezza, S.L. Marchiano, A.J. Arvia, J. Electroanal. Chem. 336 (1992) 85.
[21] D. Landolt, Electrochim. Acta 39 (1994) 1075.
[22] A.J. Bard, L.R. Faulkner, Electrochemical Methods—Fundamentals and Applications, J. Wiley & Sons, New York, 1993.
[23] A.M.O. Brett, C.M.A. Brett, Electroquímica—Princípios, Métodos e Aplicações, Oxford University Press, New York, 1993.